© 2015. Published by The Company of Biologists Ltd | Development (2015) 142, 3721-3733 doi:10.1242/dev.127589

RESEARCH ARTICLE

# Modulating the expression level of secreted Wnt3 influences cerebellum development in zebrafish transgenics

**Cathleen Teh[1,*], Guangyu Sun[2,3,*], Hongyuan Shen[1], Vladimir Korzh[1,4,‡] and Thorsten Wohland[2,3,4,‡]**

## ABSTRACT

The boundaries of brain regions are associated with the tissue-specific secretion of ligands from different signaling pathways. The dynamics of these ligands *in vivo* and the impact of its disruption remain largely unknown. Using light and fluorescence microscopy for the overall imaging of the specimen and fluorescence correlation spectroscopy (FCS) to determine Wnt3 dynamics, we demonstrated that Wnt3 regulates cerebellum development during embryogenesis using zebrafish *wnt3* transgenics with either tissue-specific expression of an EGFP reporter or a functionally active fusion protein, Wnt3EGFP. The results suggest a state of dynamic equilibrium of Wnt3EGFP mobility in polarized neuroepithelial-like progenitors in the dorsal midline and cerebellar progenitors on the lateral side. Wnt3EGFP is secreted from the cerebellum as shown by measurements of its mobility in the ventricular cavity. The importance of Wnt secretion in brain patterning was validated with the Porcn inhibitor Wnt-C59 (C59), which, when applied early, reduced membrane-bound and secreted fractions of Wnt3EGFP and led to a malformed brain characterized by the absence of epithalamus, optic tectum and cerebellum. Likewise, interference with Wnt secretion later on during cerebellar development negatively impacted cerebellar growth and patterning. Our work, supported by quantitative analysis of protein dynamics *in vivo*, highlights the importance of membrane-localized and secreted Wnt3 during cerebellum development.

**KEY WORDS: Fluorescence correlation spectroscopy (FCS), Cerebellum, Brain ventricle, Protein fractions, Ligand, C59 Wnt inhibitor**

## INTRODUCTION

As the brain develops, cell proliferation becomes restricted to a vicinity of several signaling centers. Their signaling function and brain development henceforth are mediated by secreted ligands of several signaling pathways (Ye et al., 1998, 2001). The brain midline, one of these signaling centers, is represented dorsally by the roof plate and ventrally by the floor plate. The cells of the brain midline, along with those of the mid-diencephalic and mid-hindbrain boundaries, represent the signaling glia, which is a source of secreted factors including Wnts involved in the dorso-ventral and antero-posterior specification of the brain (Jessell, 2000; Korzh et al., 2007). The signaling glia, which possess extended soma and/or filopodia, function as a conduit of distant delivery of hydrophobic Wnts (Kondrychyn et al., 2013; Korzh, 2014; Stanganello et al., 2015).

Several zebrafish Wnt genes are expressed at the midbrain-hindbrain boundary (MHB) and roof plate (Molven et al., 1991; Krauss et al., 1992; Blader et al., 1996). Mutations affecting Wnt signaling in zebrafish illustrated an important role of canonical Wnt/β-catenin signaling during neural development (Dorsky et al., 2002; Bonner et al., 2008). Wnt signaling is required for normal brain development (Clevers and Nusse, 2012), including that of the cerebellum (Selvadurai and Mason, 2011). Cerebellar vermis hypoplasia in Joubert syndrome, for example, is linked to defective canonical Wnt signaling (Lancaster et al., 2011). Wnt3 is expressed in the developing cerebellum and the dorsal spinal cord of all vertebrates (Roelink and Nusse, 1991; Bulfone et al., 1993; Garriock et al., 2007; Clements et al., 2009; Anne et al., 2013). In mice, Wnt3 is expressed prior to gastrulation and its targeted deletion causes an early developmental arrest (Liu et al., 1999). In human, homozygous nonsense mutation within the WNT3 coding region (Q83X) resulted in the loss of all limbs with concomitant CNS, craniofacial and urogenital defects in affected fetuses (Niemann et al., 2004). Wnt3 was identified as an extracellular regulator of granule cell progenitor proliferation and differentiation during mouse cerebellar development (Anne et al., 2013). Depending on cellular context, Wnt3 either acts via the canonical Wnt pathway by activating the nuclear translocation of β-catenin (Kim et al., 2008), or via the RhoA pathway (Kobune et al., 2007).

Secretion of Wnts is of particular interest because of a role of excessive production of Wnts in oncogenesis (Nusse and Varmus, 1982, 2012). Assessing levels of Wnt activity and modulating this activity *in vivo* can be achieved using a combination of fluorescent transgenic reporters and inhibitors of Wnt signaling (Yin et al., 2012; Anastas and Moon, 2013; Proffitt et al., 2013). To study the role of Wnt3 in development, zebrafish *wnt3* transgenics were generated, which expressed, in the developing cerebellum, a Wnt3-EGFP fusion protein or EGFP reporter under control of a 4 kb *wnt3* promoter. This opened up the possibility to investigate Wnt3 mobility *in vivo* using fluorescence correlation spectroscopy (FCS), as shown for teleost embryos (Pan et al., 2007b; Ries et al., 2009) and the *Drosophila* wing (Zhou et al., 2012). Results obtained from FCS analysis include determination of diffusion coefficients in cytosolic as well as membrane-associated fractions of EGFP-labeled proteins (Shi et al., 2009; Yu et al., 2009; Muller et al., 2013). The same approach was used here to define the intracellular and extracellular populations of Wnt3 and effects of two different Wnt inhibitors, C59 (Proffitt et al., 2013; Stewart et al., 2014) and IWR-1 (Lu et al., 2009; Yin et al., 2012), on Wnt3 population distribution and function. The aim of this research was to study protein dynamics *in vivo* (Pan et al., 2007a; Mütze et al., 2011; Foo et al., 2012; Macháň and Wohland, 2014)

[1]Institute of Molecular and Cell Biology, Agency for Science, Technology and Research, Singapore, 138673 Singapore. [2]Department of Chemistry, National University of Singapore, 117543 Singapore. [3]Center for Bioimaging Sciences, National University of Singapore, 117557 Singapore. [4]Department of Biological Sciences, National University of Singapore, 117543 Singapore.
*These authors contributed equally to this work

‡Authors for correspondence (vlad@imcb.a-star.edu.sg; twohland@nus.edu.sg)

**Received 16 June 2015; Accepted 28 August 2015**

Development (2015) 142, 3721-3733 doi:10.1242/dev.127589

and associate it with cerebellum development and growth. Our results demonstrate the importance of membrane-localized and secreted Wnt3 in regulation of cerebellar development.

## RESULTS

### Tg(*wnt3*:EGFP) is a faithful reporter of Wnt3 expression

The expression pattern of zebrafish *wnt3* has been described (Clements et al., 2009). To begin deciphering the role of Wnt3 in neural development, two DNA regulatory fragments, 2 kb and 4 kb in length, 5′ upstream from the translational start site of *wnt3*, were PCR-amplified using zebrafish BAC (CR450820.4) as a template. The PCR product was sub-cloned into a promoterless EGFP vector (pEGFP-1). Transient transgenesis carried out by panembryonic injection of either plasmid into 1- to 2-cell-stage zebrafish embryos detected promoter activity from the 4 kb fragment. Transgenic lines were generated using the modified Tol2 transposon system. The 4 kb-EGFP fragment was sub-cloned into a miniTol2 vector (Balciunas et al., 2006) and injected into embryos. Several independent transgenic lines, differing in the intensity of EGFP expression with expression patterns similar to that of *wnt3*, were generated. Tg(-4.0*wnt3*:EGFP)$^{F1}$ transgenics were used for the remainder of this study.

To determine whether Tg(-4.0*wnt3*:EGFP)$^{F1}$ faithfully reports *wnt3* transcription at different developmental stages, we compared *in vivo* images of EGFP expression with that of *wnt3* between 24 and 72 hours post fertilization (hpf) (Fig. 1A). The spatio-temporal profile of EGFP expression in the ventral epithalamus, roof plate, optic tectum, floor plate, MHB, cerebellum and hindbrain closely mimics that of *wnt3* (24-72 hpf; Fig. 1A-J). The co-immunohistochemical detection of EGFP and the neuronal marker HuC/D on cross sections of 48 hpf embryos (Fig. 1G-J) indicated that EGFP$^{+}$ domains in the roof plate, tegmental floor plate and cerebellum are flanked by HuC/D-positive neurons and do not express this differentiation marker. This suggests that EGFP-expressing cells are committed to a non-neuronal fate. Hence, the 4 kb *wnt3*-promoter contains most, if not all, regulatory elements and allows *in vivo* detection of Wnt3 expression.

### Wnt3EGFP is expressed in domains of endogenous *wnt3*

To facilitate the analysis of Wnt3 function *in vivo*, the same promoter was used to generate transgenics expressing the functionally active Wnt3 fusion protein, Wnt3EGFP. The functional activity of the fusion protein was first verified in zebrafish embryos. The *wnt3*:*egfp* fusion cassette was cloned downstream of the constitutively active cytomegalovirus (CMV) promoter. The panembryonic overexpression of this construct led to malformed eyes and posteriorized CNS, i.e. the phenotype associated with ectopic Wnt signaling (van de Water et al., 2001). This indicated that recombinant Wnt3EGFP retains Wnt3 activity (Fig. S1A).

The CMV promoter was replaced with the 4 kb *wnt3* promoter and the resulting construct (-4.0*wnt3*:Wnt3EGFP) was used to generate zebrafish transgenics, e.g. Tg(-4.0*wnt3*:Wnt3EGFP)$^{F1}$ and Tg(-4.0*wnt3*:Wnt3EGFP)$^{F2}$, with spatio-temporal expression of EGFP identical to that of the reporter line Tg(-4.0*wnt3*:EGFP)$^{F1}$ (Fig. 2A-O). This expression is temporally regulated. Both EGFP and Wnt3EGFP were first detected in polarized neuroepithelial cells of the dorsal midline in the optic tectum, cerebellum and the cerebellar rhombic lip, one of the germinal zones in the cerebellum (Hashimoto and Hibi, 2012) (Fig. 2A,F,K). Expression of both is enhanced by 36 hpf and reduces by 4 days post fertilization (dpf) (Fig. 2P-V). The only exception was Tg(-4.0*wnt3*:Wnt3EGFP)$^{F3}$, in which expression started relatively late (36 hpf) and remained high in the developing cerebellum (Fig. 2W). The four different transgenic lines of zebrafish expressing EGFP or Wnt3EGFP fusion protein in the cerebellum are henceforth referred to as Tg(*wnt3*:EGFP)$^{F1}$, Tg(*wnt3*:Wnt3EGFP)$^{F1}$, Tg(*wnt3*:Wnt3EGFP)$^{F2}$ and Tg(*wnt3*:Wnt3EGFP)$^{F3}$.

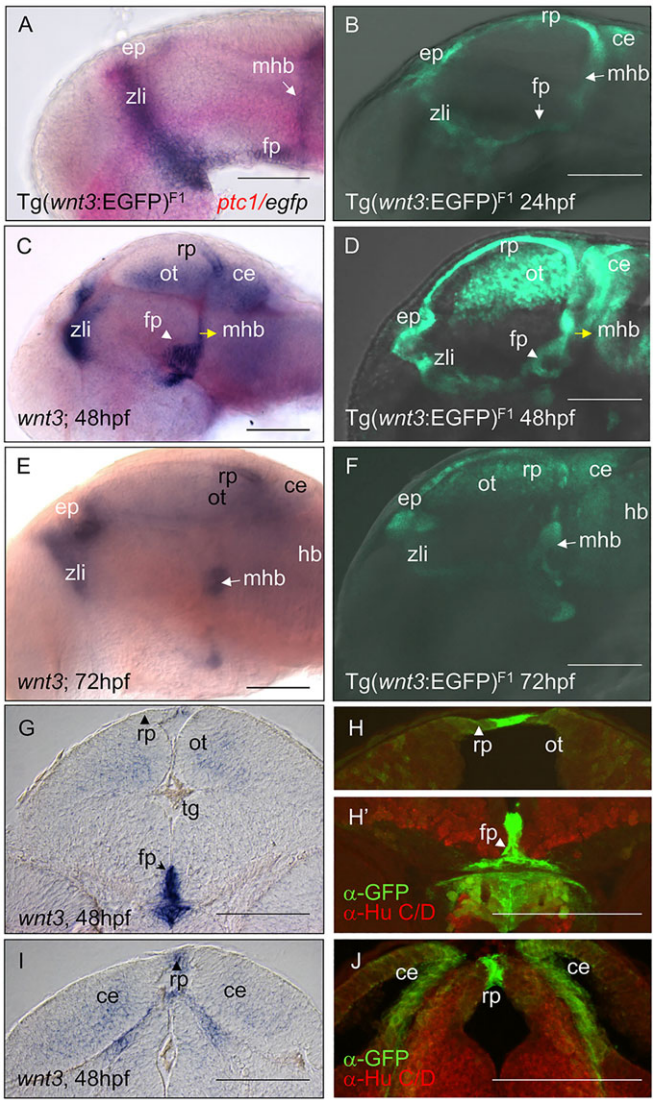


**Fig. 1. EGFP and Wnt3 expression in transgenics under control of the *wnt3* promoter.** A stable zebrafish transgenic line containing the 4 kb *wnt3* promoter drives EGFP expression in a *wnt3*-like manner with spatio-temporal correlation with endogenous transcripts. (A) *egfp* transcript expression (purple) in 4 kb *wnt3* promoter transgenic line Tg(-4.0*wnt3*:EGFP)$^{F1}$ colocalized with *ptc1* (pink) at the zona limitans intrathalamica (zli) at 24 hpf. (B) An *in vivo* image of 24 hpf Tg(-4.0*wnt3*:EGFP)$^{F1}$ showing EGFP$^{+}$ domains highlighted by the transgenic line. (C,E) *wnt3* transcripts (purple) are detected in the cerebellum (ce), epithalamus (ep), floor plate (fp), optic tectum (ot), roof plate (rp), midbrain hindbrain boundary (mhb) and hindbrain (hb) of larvae at 48 hpf (C) and 72 hpf (E). (D,F) *In vivo* images of Tg(-4.0*wnt3*:EGFP)$^{F1}$ at 48 hpf (D) and 72 hpf (F) showing similar EGFP$^{+}$ domains. (G-J) Comparison of midbrain (G,H) and cerebellum (I,J) cross sections of *wnt3* expression in a 48 hpf zebrafish brain (G,I) with corresponding cross sections of Tg(-4.0*wnt3*:EGFP)$^{F1}$ (H-J) that detected EGFP expression in similar regions. *wnt3*-positive domains include the optic tectum, floor plate and cerebellum. Co-immunohistochemical detection of EGFP and Hu-positive neurons showed that EGFP$^{+}$ domains in the floor plate, floor plate and cerebellum are flanked by neurons (H,H′,J). Scale bars: 100 µm.

Development (2015) 142, 3721-3733 doi:10.1242/dev.127589

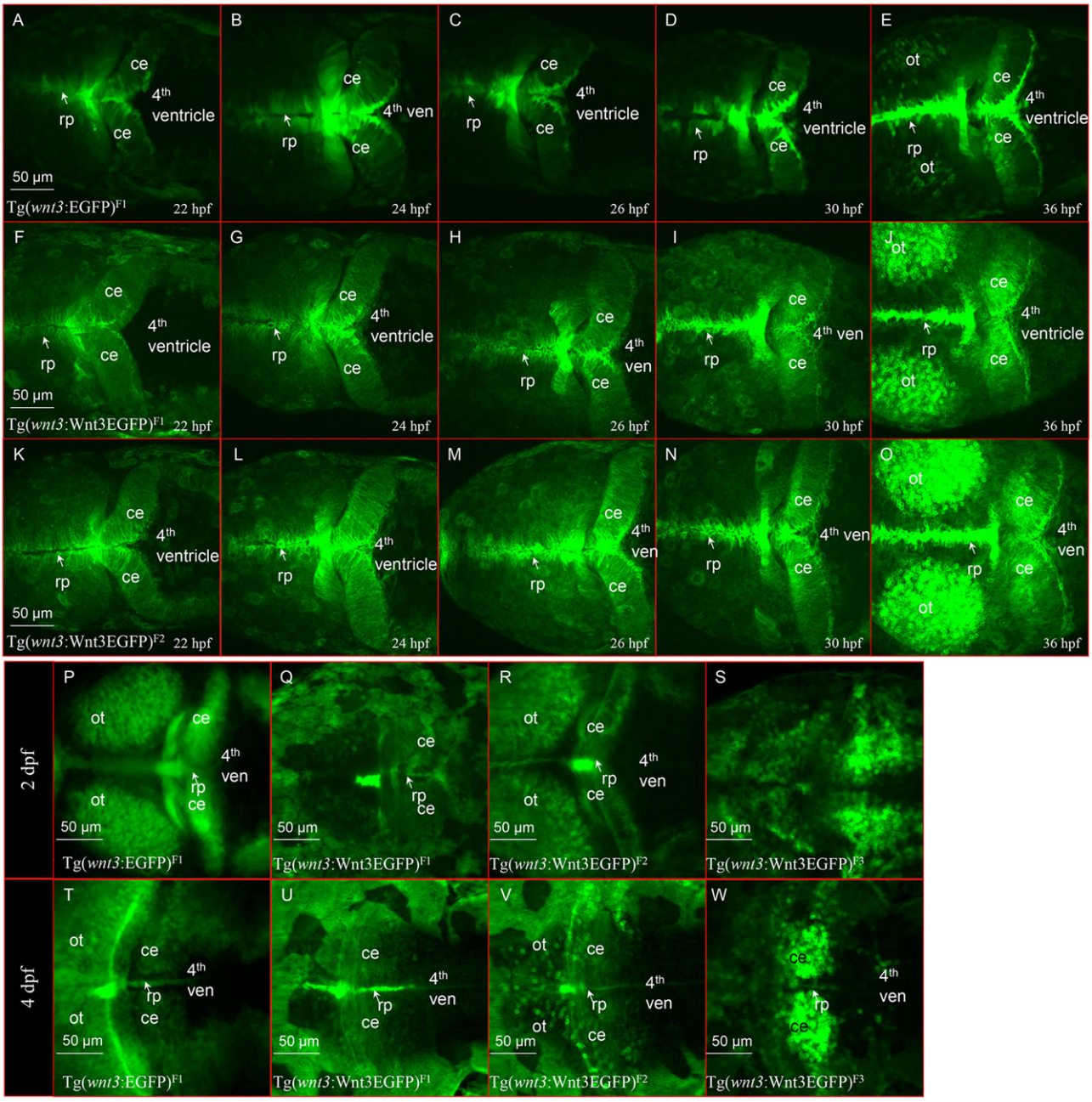


**Fig. 2. Spatio-temporal expression of *wnt3* promoter-driven EGFP/Wnt3EGFP.** Spatio-temporal expression of 4 kb *wnt3* promoter-driven EGFP/Wnt3EGFP influenced by genomic insertion of a transgene varies in strength. Tg(-4.0*wnt3*:EGFP)$^{F1}$, Tg(-4.0*wnt3*:Wnt3EGFP)$^{F1}$, Tg(-4.0*wnt3*:Wnt3EGFP)$^{F2}$ and Tg(-4.0*wnt3*:Wnt3EGFP)$^{F3}$ are abbreviated in the figure as Tg(*wnt3*:EGFP)$^{F1}$, Tg(*wnt3*:Wnt3EGFP)$^{F1}$, Tg(*wnt3*:Wnt3EGFP)$^{F2}$ and Tg(*wnt3*:Wnt3EGFP)$^{F3}$, respectively. (A-O) Initial spatio-temporal similarity of expression of EGFP and Wnt3EGFP is maintained in three independent transgenic lines. (P-W) Tg(-4.0*wnt3*:Wnt3EGFP)$^{F3}$ maintains strong Wnt3EGFP expression in the cerebellum beyond 48 hpf. Transgene expression in the optic tectum and cerebellum decreases from 48 hpf in all other Wnt3 transgenics. 4$^{th}$ ven, fourth ventricle; ce, cerebellum; ot, optic tectum; rp, roof plate.

### Functional Wnt3EGFP positively regulates flanking tissue growth in the MHB and the cerebellum

The impact of spatio-temporal control of Wnt3 dosage on flanking tissue growth was assessed in living zebrafish using Tg(memKR15-16), which expresses the membrane-tethered fluorescent protein KillerRed (KR). This transgenic line traps the expression of the zebrafish gene *eng1b* (Kondrychyn et al., 2011), an ortholog of mouse *En1*. Both *Wnt3* and *En1* transcripts are detected in the embryonic mouse MHB and the cerebellum (Millen et al., 1995). Similarly in the *eng1b*-trapped transgenic zebrafish, KillerRed expression in the MHB and the cerebellum overlaps with and flanks Wnt3EGFP expression in Tg(*wnt3*:Wnt3EGFP) families. Histological characterization of Tg(*wnt3*:Wnt3EGFP)$^{F2}$ in the background of Tg(memKR15-16) confirmed Wnt3EGFP expression in the cerebellum, where Wnt3EGFP cells are predominantly localized to the upper rhombic lip (Fig. S2D-G), a proliferative niche containing progenitor cells even in adult fish (Kaslin et al., 2013). Most of the Wnt3EGFP detected by immunohistochemistry accumulates in the plasma membrane of expressing cells, mimicking *in vivo* expression detected in transgenics. All Wnt3EGFP-positive cells of the cerebellum were negative for the neuronal marker HuC/D at 3 dpf

Development (2015) 142, 3721-3733 doi:10.1242/dev.127589

(Fig. S2D,E). All Wnt3EGFP-expressing cells in the ventral MHB adopted distinctly radial glia-like morphology, with cell bodies located within the luminal aspect of the ventricular wall and a primary process extending into the subventricular zone (Fig. S2B,C,F,G). The glial identity of these cells was confirmed by immunodetection of glial fibrillary acidic protein (GFAP). Colocalization of some Wnt3EGFP cells with BrdU-positive replicating cells in the cerebellum (Fig. S2F-G) confirms their localization to a proliferation niche.

The role of Wnt3 in inhibiting proliferation of cultured cerebellar granule progenitors and regulating its neurogenesis has been documented in mice (Anne et al., 2013). We investigated whether a similar role exists for Wnt3 by assessing its impact on cerebellum neurogenesis in zebrafish. In the absence of a zebrafish *wnt3* mutant, a functional analysis was conducted using the morpholino phosphodiamidate antisense oligonucleotides (MO)-mediated loss-of-function (LOF) approach. Knockdown of Wnt3 was achieved by interfering with pre-mRNA splicing at the exon1-intron1 boundary (MO1) or inhibition of mRNA translation by targeting the *wnt3* 5′-UTR (MO2) (Fig. S3A). RT-PCR with *wnt3*-specific primers showed that microinjection of MO1 successfully interfered with *wnt3* splicing such that no wild-type *wnt3* transcripts could be detected in 30 hpf embryos after MO1 injection (Fig. S3B). MO2 anneals to a 25 bp sequence in the *wnt3* 5′-UTR which is also present in the 4 kb *wnt3* upstream promoter that drives reporter expression in Wnt3 stable transgenics. The specificity of MO2 was verified by microinjecting into Tg(*wnt3*:EGFP)$^{F1}$, where interference of EGFP translation upon binding of MO2 to the *wnt3* 5′-UTR upstream of the EGFP reporter was documented. EGFP intensity is similar in wild-type (WT) controls and Tg(*wnt3*:EGFP)$^{F1}$ MO1 morphants (Fig. S3C-E), but reduced in MO2 morphants (Fig. S3F-G). To eliminate undesirable off-target effects (Robu et al., 2007) of *wnt3* MOs, concurrent p53 and Wnt3 knockdown was performed. The effect of Wnt3 knockdown on cerebellar neurogenesis was examined using zebrafish HuC transgenics, Tg(*elav3*:GFP), in which GFP labels all neurons (Park et al., 2000). GFP expression in both WT and Wnt3 morphants at 3 dpf was compared (Fig. S3C-L) and microinjection of either MO1 or MO2 morphants, with or without p53 MO, consistently reduces GFP-positive neurons in the cerebellum (Fig. S3H-L, enlarged white box) of Tg(*elav3*:GFP) morphants. This suggests that zebrafish *wnt3* plays an essential role in cerebellar neurogenesis.

We further investigated the impact of Wnt3 dosage on cerebellum development. The cerebellum is located at the dorsal-most part of the anterior hindbrain, posterior to the MHB. Volumetric assessment of *eng1b*-trapped MHB and cerebellum in Tg(*wnt3*:EGFP) or Tg(*wnt3*:Wnt3EGFP) families was performed to determine the impact of Wnt3 dosage on growth of KR-marked domains in Tg(memKR15-16) transgenics (Fig. 3A-C). Double transgenics Tg(memKR15-16)/Tg(*wnt3*:EGFP)$^{F1}$ were used as a control group expressing normal level of Wnt3. Double transgenic Tg(*wnt3*:Wnt3EGFP)$^{F2}$ larvae displayed intermediately elevated Wnt3 expression and Tg(*wnt3*:Wnt3EGFP)$^{F3}$ displayed high Wnt3 expression. Volumetric analysis of the KillerRed-positive brain segment (MHB and cerebellum) at 4 dpf demonstrated that Tg(*wnt3*:Wnt3EGFP)$^{F3}$ had on average a 22% larger memKR-positive domain compared with controls (Fig. 3D; $P$=0.0022). The positive correlation between *in vivo* Wnt3EGFP dosage and brain volume suggests that Wnt3EGFP is functional and positively regulates growth of the MHB and cerebellum.

The ability of bioactive Wnt3EGFP to compensate for a lack of endogenous Wnt3 activity after MO1-meditated knockdown

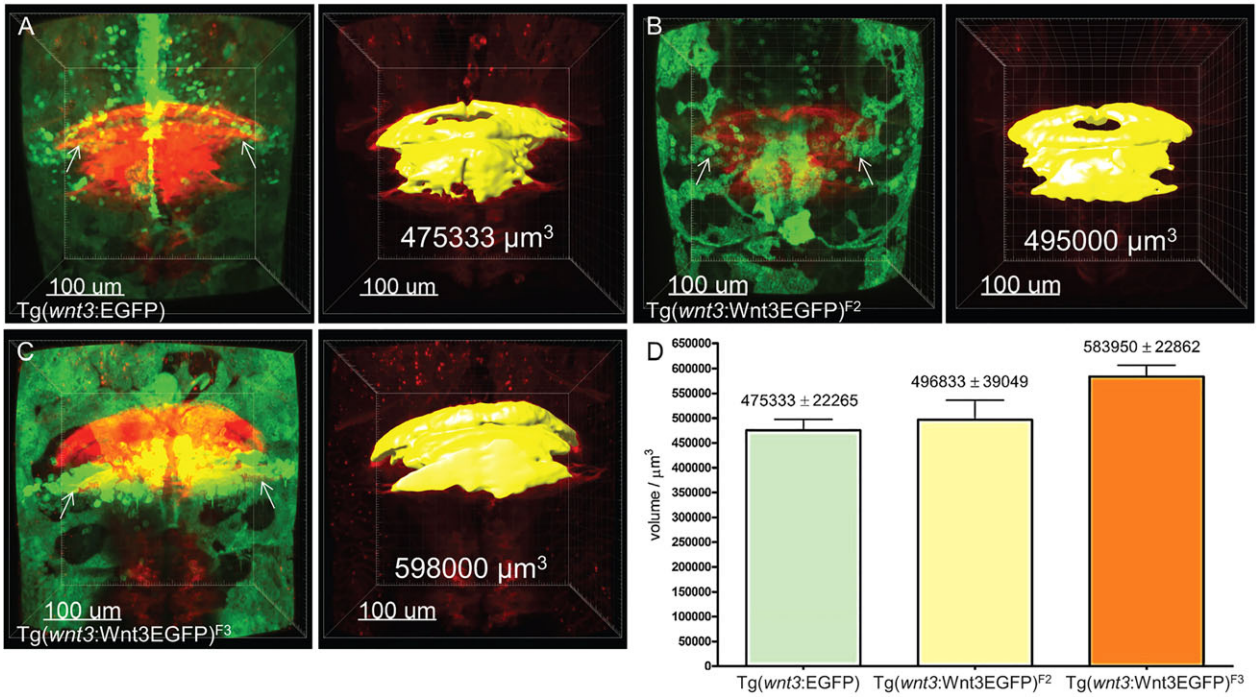


**Fig. 3. The size of the MHB and cerebellum segmental volume correlates with the level of Wnt3EGFP expression.** (A-C) *In vivo* comparison of segmental volume in Tg(memKR15-16) in EGFP or different Wnt3EGFP transgenics background at 4 dpf. Tg(memKR15-16)/EGFP (A), Tg(memKR15-16)/Wnt3EGFP [Tg(*wnt3*:Wnt3EGFP)$^{F2}$] (B) and Tg(memKR15-16)/Wnt3EGFP [Tg(*wnt3*:Wnt3EGFP)$^{F3}$] (C). KillerRed expression in the MHB and cerebellum of Tg(memKR15-16) is in red; EGFP or Wnt3EGFP expression in *wnt3* transgenics is in green; and yellow represents a 3D view of the computed volume. (D) The increase in segmental volume in Tg(memKR15-16) is significant according to unpaired *t*-test comparing Tg(*wnt3*:EGFP)$^{F1}$ vs Tg(*wnt3*:wnt3EGFP)$^{F3}$ ($P$=0.0022). Arrows show expression of EGFP/Wnt3EGFP in the cerebellum.

Development (2015) 142, 3721-3733 doi:10.1242/dev.127589

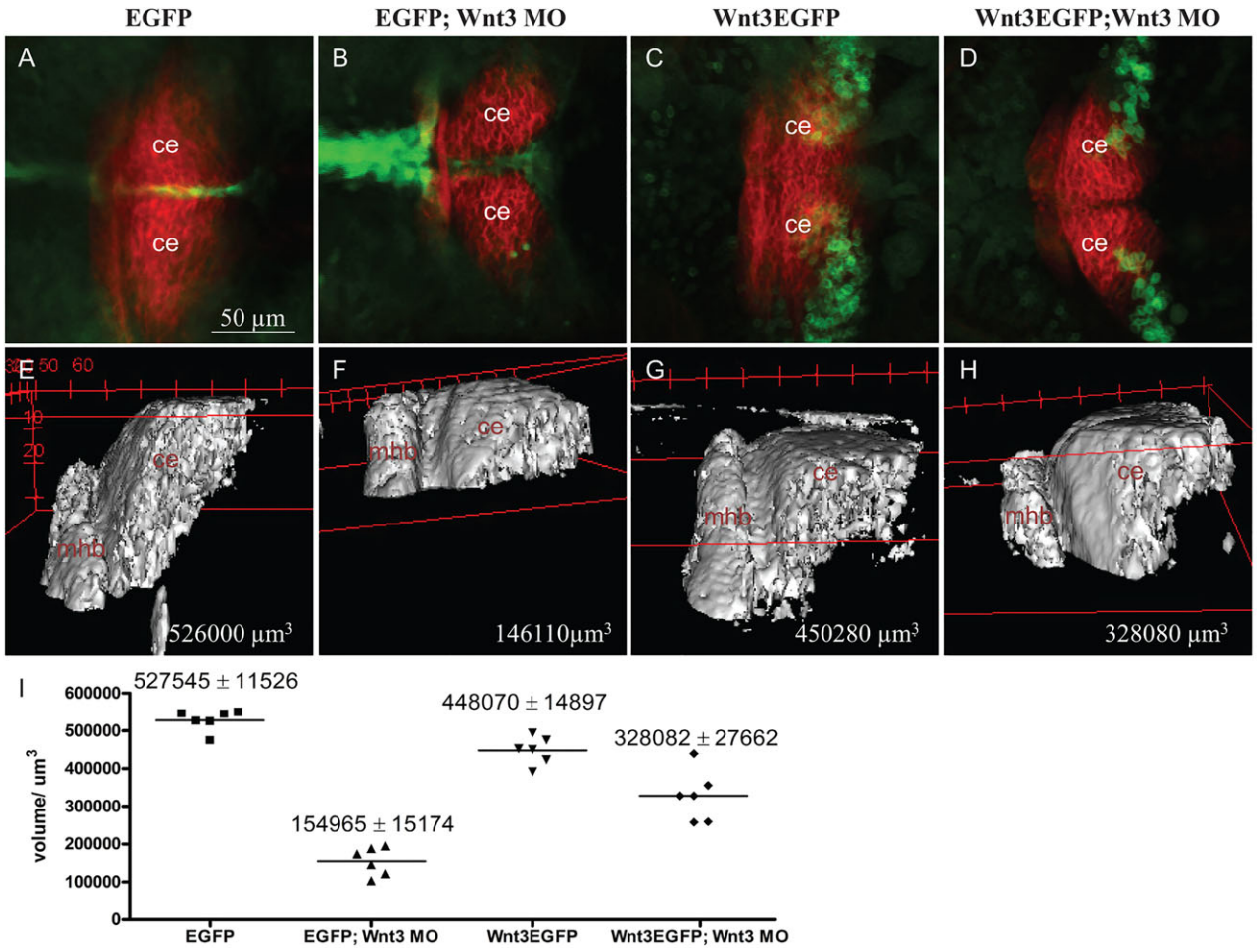


**Fig. 4. Expression of Wnt3EGFP in the cerebellum of Tg(*wnt3*:Wnt3EGFP)$^{F3}$ partially compensates cerebellum growth in MO1-injected Wnt3 morphants.** (A-D) Dorsal view of double transgenic Tg(memKR15-16) larvae co-expressing KillerRed with EGFP from Tg(*wnt3*:EGFP)$^{F1}$ (A,B) or Wnt3EGFP from Tg(*wnt3*:Wnt3EGFP)$^{F3}$ (C,D). KillerRed is expressed in the MHB and cerebellum. Reduction in KillerRed-positive cerebellum is partially compensated in 3 dpf Tg(*wnt3*:Wnt3EGFP)$^{F3}$ MO1-morphants (D). (E-H) 3D lateral view of KillerRed-positive MHB and cerebellum in Tg(*wnt3*:EGFP)$^{F1}$ (E), MO1-injected Tg(*wnt3*:EGFP)$^{F1}$ (F), Tg(*wnt3*:Wnt3EGFP)$^{F3}$ (G) and MO1-injected Tg(*wnt3*:Wnt3EGFP)$^{F3}$ at 3 dpf (H). (I) Scatter plot of computed volumes. The decrease in segmental volume in Tg(memKR15-16) is significant between MO1-morphants and un-injected siblings. Unpaired *t*-test comparing Tg(*wnt3*:EGFP)$^{F1}$ vs MO1-morphant Tg(*wnt3*:EGFP)$^{F1}$, $P<0.0001$; Tg(*wnt3*:wnt3EGFP)$^{F3}$ vs MO1-morphants Tg(*wnt3*:Wnt3EGFP)$^{F3}$, $P=0.0034$. Segmental volume in MO1-morphant Tg(*wnt3*:Wnt3EGFP)$^{F3}$ remains significantly higher than in MO1-morphant Tg(*wnt3*:EGFP)$^{F1}$ ($P=0.0003$). ce, cerebellum; mhb, midbrain hindbrain boundary.

was confirmed in double transgenics of Tg(memKR15-16) larvae expressing either EGFP or Wnt3EGFP (Fig. 4). Tg(*wnt3*:Wnt3EGFP)$^{F3}$ expresses endogenous Wnt3 and Wnt3EGFP whereas the Wnt3 reporter Tg(*wnt3*:EGFP)$^{F1}$ serves as a control expressing only endogenous Wnt3. Since MO1 interferes with the formation of mature *wnt3* transcripts in all injected larvae, the cerebellum in Tg(*wnt3*:EGFP)$^{F1}$ and Tg(*wnt3*:Wnt3EGFP)$^{F3}$ Wnt3 morphants are significantly smaller than un-injected siblings (Fig. 4I, $P<0.0001$ and $P=0.0034$, respectively). Nevertheless, Wnt3 morphants of Tg(*wnt3*:Wnt3EGFP)$^{F3}$ have a significantly bigger cerebellum than their Tg(*wnt3*:EGFP)$^{F1}$ counterparts (Fig. 4I, $P=0.0003$) as a result of additional Wnt3EGFP expression in the cerebellum. We further assessed whether the decreased brain volume observed in Wnt3 morphants is attributed to a change in cell size or cell numbers. Concurrent with the experiments already described, the same sample sets were analyzed for cell size (cell area), taking ten random cells from a morphologically similar optical slice of the cerebellum. Cell area was measured using ImageJ software. No significant difference in cell size was detected in Wnt3 morphants when compared with controls (Fig. S4). Hence, Wnt3-linked changes in cerebellum volume results in alteration of cell numbers rather than cell size.

### Characterization of Wnt3EGFP membrane dynamics *in vivo*

Wnt3EGFP must be secreted in a manner comparable to endogenous Wnt3 to function properly. Confocal microscopy showed that Wnt3EGFP was transported to the plasma membrane. FCS was instrumental in determining diffusion coefficients of cytosolic as well as membrane-tethered EGFP-labeled proteins (Shi et al., 2009). The mobility of secreted ligands in the extracellular space could be involved in generation of the morphogen gradient in developing zebrafish (Yu et al., 2009). Hence, we decided to characterize the distribution of Wnt3EGFP at the plasma membrane using FCS. Tg(*wnt3*:Wnt3EGFP)$^{F2}$ transgenic embryos were used to detect Wnt3EGFP by FCS in the cerebellum. Fig. 5A shows a typical autocorrelation curve measured on the plasma membrane. The experimental data was fitted to a model, which was determined by Bayes inference-based model selection (Guo et al., 2012; Sun et al., 2015). The model accounts for two diffusive particles and also a possible triplet state of the fluorophore (Eqn 13 in the supplementary Materials and Methods). A significant fraction of

Development (2015) 142, 3721-3733 doi:10.1242/dev.127589

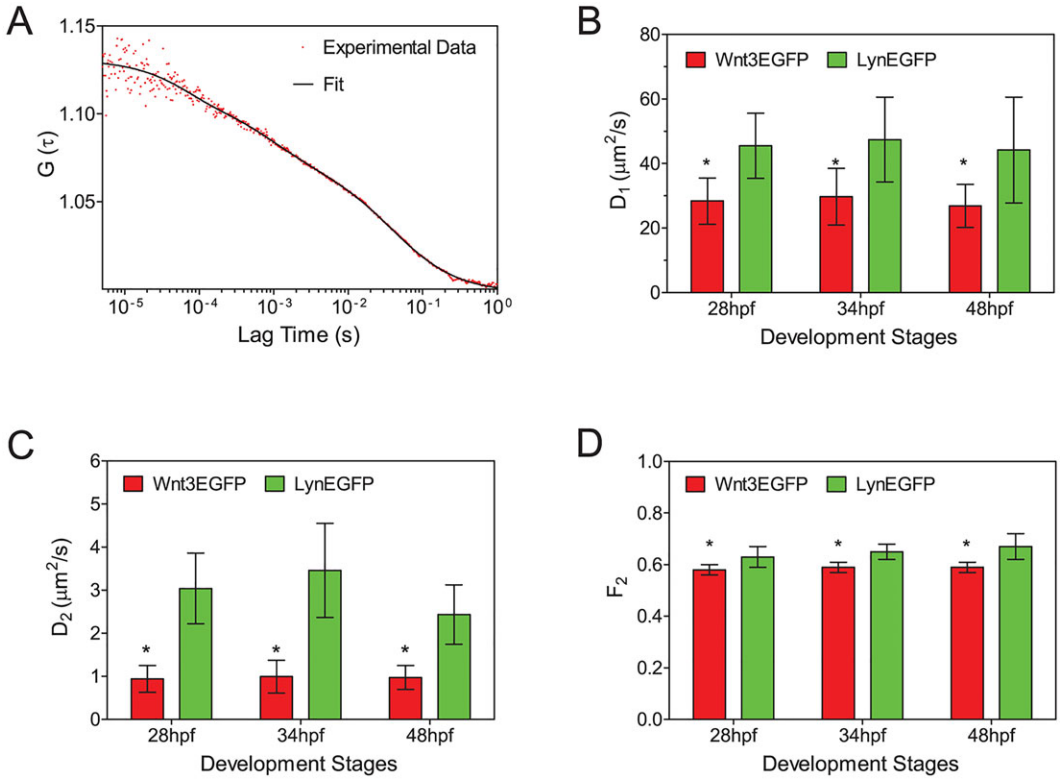


**Fig. 5. FCS analysis of Wnt3EGFP and LynEGFP membrane dynamics in the cerebellum.** (A) Autocorrelation curve of Wnt3EGFP on the plasma membrane. The curve is fitted into a two-component model including a blinking process. Dots represent the experimental data. Solid line is the fit curve. (B,C) Diffusion coefficients ($D_1$, $D_2$) extracted from fit at different development stages. (D) Fraction of slow-migrating component ($F_2$) extracted from fit at different developmental stages. The difference in membrane fraction of LynEGFP and Wnt3EGFP indicates the existence of a small amount of intercellular Wnt3EGFP. Data are mean±s.d. Red bar, Wnt3EGFP; green bar, LynEGFP. Significance level, two-way *t*-test, **P*<0.001. See also Fig. S1 and Table S1.

the protein detected (60%, fraction $F_2$) was represented by a membrane-tethered component with a diffusion coefficient ($D_2$) ~1 μm$^2$/s. This fraction could be present either in cells secreting Wnt3 and/or in cells receiving Wnt3. The rest of the signal (40%) was represented by a fast-moving component with diffusion coefficient $D_1$~30 μm$^2$/s. This fast-moving component has a similar, though slightly lower, diffusion coefficient to that of cytosolic EGFP in Tg(-4.0*wnt3*:EGFP)$^{F2}$ (abbreviated EGFP$^{F2}$, see Table S1). A lower diffusion coefficient is expected because of the difference in molecular mass between Wnt3EGFP and cytosolic EGFP. In addition, considering the possibility of post-translational modification of Wnts by lipids, the fast component could be in a soluble complex with other partner(s) (Willert et al., 2003), further lowering the diffusion coefficient.

We tested whether the protein dynamics varies in different parts of the cerebellum, such as between polarized neuroepithelial-like progenitors in the dorsal midline (DM) and cerebellar progenitors on the lateral side (LS) during development. Measurements were performed in these two regions at 28, 34 and 48 hpf (Fig. S5A). The results showed that Wnt3EGFP mobility and its membrane distribution ($F_2$) in Tg(*wnt3*:Wnt3EGFP)$^{F2}$ remains relatively constant in both regions of the cerebellum throughout this period (Fig. S5C-E). The data were also analyzed using fluorescence intensity to detect cells with different expression, but again, no significant difference in Wnt3EGFP membrane distribution ($F_2$) was detected (Fig. S5F). These data suggest that Wnt3 fractions are in a stable dynamic equilibrium during cerebellum development.

As a negative control, we also assayed the distribution of LynEGFP, a tracer membrane-tethered protein, which, being non-secreted, remains in the cell. Compared with Wnt3EGFP, the mobility of both the fast- and slow-moving components of LynEGFP are of the same order of magnitude, although slightly higher in LynEGFP (Fig. 5B,C). This suggests that the fast Wnt3 component represents intracellular Wnt3EGFP. As the nucleus occupies most of the cell volume during this period of development, both components are detected near the plasma membrane (Fig. S5B). Expression level does not influence LynEGFP dynamics, similar to observations for Wnt3EGFP (Fig. S5F). However, the membrane fraction ($F_2$) of Wnt3EGFP is ~5% smaller than that of LynEGFP (Fig. 5D; Fig. S5F) suggesting that this amount probably represents secreted Wnt3EGFP. To analyze this fraction we measured Wnt3EGFP in the brain ventricle adjacent to Wnt3-expressing cells.

### Characterization of Wnt3EGFP dynamics in the brain ventricle

The small size of extracellular space in tissue makes it difficult to further characterize the extracellular fraction of Wnt3EGFP. Fortunately, the fourth brain ventricle is directly adjacent to Wnt3-expressing cells in the cerebellar rhombic lip. Hence, we analyzed changes in fluorescence intensity at an axis perpendicular to the border of the cerebellum into the fourth ventricle in animals expressing Wnt3EGFP, LynEGFP or a secreted version of EGFP (secEGFP) (Fig. 6A; Fig. S6). Measurements along this axis from the cerebellum boundary into the brain ventricle were performed at the level indicated by the white arrow in Fig. 6B. Intensity was normalized to the highest point, which for Wnt3EGFP- and LynEGFP-expressing cells corresponds to the plasma membrane. To show a distribution of secreted proteins, secEGFP was used as a

Development (2015) 142, 3721-3733 doi:10.1242/dev.127589

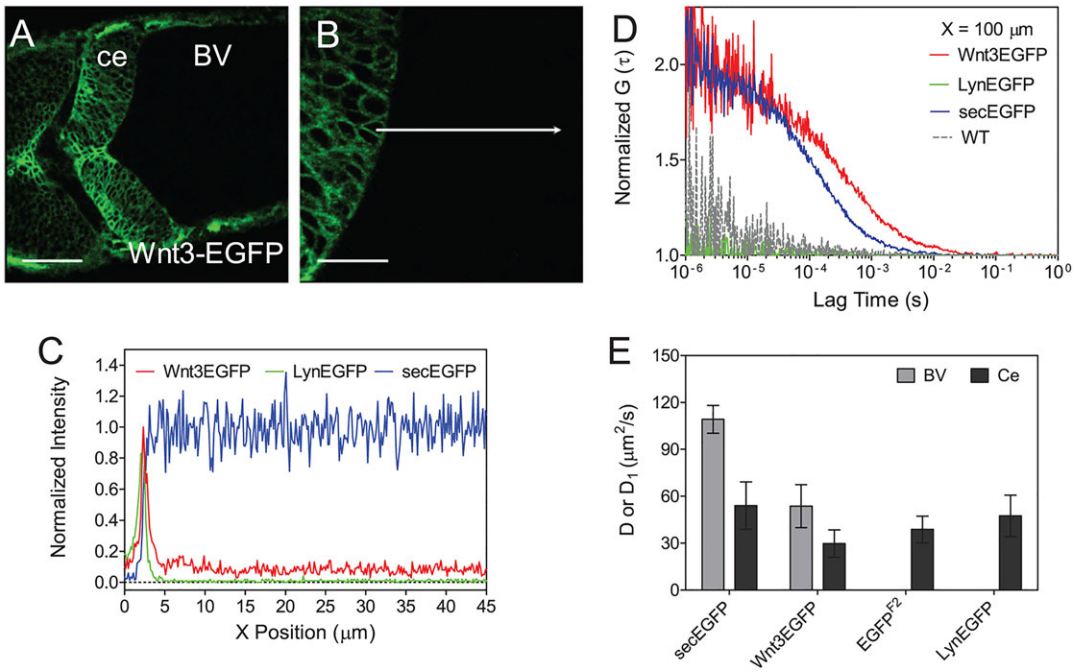


**Fig. 6. Wnt3EGFP, LynEGFP and secEGFP in the fourth brain ventricle.** (A) Confocal image of zebrafish cerebellum expressing Wnt3EGFP at 34 hpf. Scale bar: 50 µm. (B) Zoom of A at 3× magnification with focus on the cerebellum boundary and flanking brain ventricle. Scale bar: 20 µm. Images were taken in dorsal view. BV, brain ventricle; ce, cerebellum. The images were modified using Imaris to increase the contrast. (C) Normalized fluorescence intensity from the cerebellum boundary cell to the brain ventricle along the white arrow in B of Wnt3EGFP (red), LynEGFP (green) and secEGFP (blue). Data are the average of three scans of three embryos for each type to the highest point. (D) Normalized ACF curves taken within a ventricle at 100 µm from the cerebellum boundary. Color-coding is the same as in C together with wild type (WT, dotted gray). The results show the free diffusion of Wnt3EGFP and secEGFP in the brain ventricle, whereas no fluorescence can be detected either for LynEGFP or for WT. (E) Diffusion coefficients extracted from fit for different types of EGFP-labeled proteins in both the cerebellum and the brain ventricle. secEGFP serves as an intercellular indicator of protein mobility in multicellular tissue and extracellular indicator in the brain ventricle. EGFP reporter Tg(-4.0*wnt3*:EGFP)$^{F2}$ and LynEGFP transgenics Tg(-*8.0cldnB*:lynEGFP) serve as an indicator of intracellular protein mobility. Data are mean±s.d. Light gray bar, brain ventricle (BV); dark gray bar, cerebellum (ce). See also Fig. S2 and Tables S2, S3.

marker in combination with KillerRed (see Materials and Methods) where membrane-tethered KillerRed expression in the cerebellum of Tg(memKR15-16) demarcates the cerebellum boundary flanking the brain ventricle (Kondrychyn et al., 2011). The profile of secEGFP distribution was normalized to the average intensity in the brain ventricle (see details in Materials and Methods). In parallel, it was also found that, consistent with previously estimated low level secretion inferred from the membrane distribution in Tg(*wnt3*:Wnt3EGFP)$^{F2}$, a moderate but significant increase of Wnt3EGFP fluorescence was present in the brain ventricle. This indicated that Wnt3EGFP is secreted and released into the brain ventricle, which was not the case for LynEGFP (Fig. 6C). Furthermore, FCS was applied to determine the extracellular mobility of Wnt3EGFP by taking measurements in the brain ventricle at a distance of 100 µm from the cerebellum edge. Autocorrelation curves show that Wnt3EGFP diffuses freely in a similar manner to secEGFP, whereas no fluorescence in this area was detected in LynEGFP or negative control embryos (Fig. 6D). These results confirm secretion of Wnt3EGFP into the brain ventricle and support the existence of an extracellular fraction of Wnt3EGFP.

FCS was used to measure protein mobility in different regions of the brain (Fig. 6E; Table S2). The mobility of secEGFP measured in the cerebellum largely represents that of extracellular protein, which is on average 50% lower compared with the mobility of Wnt3EGFP secreted into the brain ventricle. The values defining the mobility of cytosolic EGFP and that of the fast-moving component of LynEGFP represent the mobility of intracellular protein, which is slightly lower than that of extracellular protein. In addition, an extra slow component of Wnt3EGFP, with diffusion coefficients of 0.5-15 µm$^2$/s, was detected in the brain ventricle (Fig. S6B). This component represented 3-30% of all Wnt3EGFP (Fig. S7C). This is in contrast to secEGFP, which exhibits only a single component in the brain ventricle (Guo et al., 2012; Sun et al., 2015). Measurements of Wnt3EGFP mobility in the ventricular cavity not only supported the idea of a secreted fraction, but also demonstrated its release from the plasma membranes of Wnt3EGFP$^+$ cerebellar progenitors into the flanking fourth brain ventricle. In addition, these results support the presence of a very slow-migrating secreted fraction. Thus, these measurements demonstrate the presence of three fractions of Wnt3EGFP: a fast-migrating intracellular fraction, a slow-migrating membrane fraction and a secreted fraction, which itself consists of fast- and slow-migrating components.

### Block of Porcupine affects Wnt3EGFP secretion

It has been reported that Porcupine (Porcn), a membrane-bound O-acyl transferase, is necessary for the anchoring of Wnts to the cell membrane in Wnt-producing cells (Tanaka et al., 2000). In the absence of Porcn activity, Wnts are less hydrophobic and accumulate in the endoplasmic reticulum (ER). We used the Porcn inhibitor Wnt-C59 (C59) to reveal the role of Wnt secretion in the formation of distinct intra- and extracellular fractions of Wnt3EGFP. In parallel, IWR-1, another inhibitor of Wnt signaling acting at the level of β-catenin activity in target cells, and thus not influencing secretion, was used for *in vivo* comparison of inhibitor action (Chen et al., 2009; Lu et al., 2009).

First, Tg(*wnt3*:Wnt3EGFP)$^{F2}$ embryos were soaked in 20 µM of C59. This blocked formation of the cerebellum and strongly reduced

Development (2015) 142, 3721-3733 doi:10.1242/dev.127589

Wnt3EGFP (unpublished observations). This is in line with characteristics of C59 as an inhibitor of Wnt secretion (Proffitt et al., 2013). To perform FCS, a minimal level of Wnt3EGFP expression is required. Hence, for FCS experiments, the concentration of C59 was reduced to 5 µM. The number of Wnt3EGFP-expressing cells and the level of Wnt3EGFP expression were significantly reduced (Fig. 7A), while retaining sufficient Wnt3EGFP for FCS. As a control, LynEGFP transgenics with expression in the cerebellum [Tg(*-8.0cldnB*:lynEGFP)] were used (Fig. 7B), along with the control (untreated) and 1% DMSO-treated Tg(*wnt3*:Wnt3EGFP)$^{F2}$ embryos. C59 has no effect on distribution of LynEGFP. In particular, the mobility of both fast- and slow-migrating components ($D_1$ and $D_2$, respectively) as well as the membrane distribution ($F_2$) of LynEGFP were not affected by this treatment (Fig. 7C-E), indicating that properties of the plasma membrane were not affected. By contrast, Wnt3EGFP mobility on the membrane ($D_2$) and its membrane distribution ($F_2$) varied significantly; $D_2$ increased two-fold and $F_2$ was reduced by ∼15% compared with controls (Fig. 7D,E) and Wnt3EGFP was found to be almost absent in the brain ventricle (Fig. S8). In contrast to C59 treatment, Wnt3EGFP expression and/or its secretion were not affected even at high concentration of IWR-1 inhibitor (50 µM) (Table S3; Fig. S8). The impact of C59-mediated Wnt inhibition on brain patterning was confirmed using double transgenic Tg(*wnt3*:Wnt3EGFP)$^{F2}$/Tg(memKR15-8) larvae where membrane-tethered KillerRed demarcated specific segments of the brain (epithalamus, optic tectum, cerebellum and hindbrain). Successful interference with Wnt secretion by C59 during primary neurulation, first detected by FCS at 28 hpf, correlated with a drastic reduction of Wnt3EGFP and a malformed brain characterized by the absence of epithalamus, optic tectum and cerebellum at 48 hpf (Fig. S9D). Therefore, FCS data support the hypothesis that the ratio of various fractions of Wnt3EGFP depends on efficiency of its secretion. Inhibition of Wnt secretion caused an increase in the intracellular fraction of Wnt3EGFP and a reduction of its membrane-bound fraction. The latter consequently led to defective morphological patterning of the brain confirmed 1 day after the initial FCS analysis.

### Inhibition of cerebellar Wnt3EGFP secretion reduces its segmental volume

We wanted to validate whether interference with Wnt secretion during cerebellar development negatively impacts cerebellar growth and patterning. Tg(*wnt3*:Wnt3EGFP)$^{F3}$/Tg(memKR15-16) double transgenic larvae were selected as they displayed the highest levels of Wnt3EGFP expression, resulting in the largest brain increase (Fig. 3C). Embryos were exposed to Wnt inhibitors at 36 hpf, after the onset of Wnt3EGFP expression in Tg(*wnt3*:Wnt3EGFP)$^{F3}$, and treatment stopped at 72 hpf. The EGFP reporter represents embryos with endogenous level of Wnt3, i.e. negative control (Fig. 8A). Tg(*wnt3*:Wnt3EGFP)$^{F3}$ embryos treated with 1% DMSO represent a positive control (Fig. 8B). Embryos were treated with Wnt inhibitors (C59 or IWR-1) by whole embryo soaking (Fig. 8C,D). Wnt3 activity is required after 36 hpf for cerebellar development as exposure to either C59 (Fig. 8C) or IWR-1 (Fig. 8D) resulted in brain reduction. The decrease caused by IWR-1 is small (∼9%) unlike that caused by C59, administration of which led to the cerebellum size being reduced by almost half ($P$=0.0001) when compared with the positive control (Fig. 8E). This decrease in brain segmental volume is accompanied by accumulation of Wnt3EGFP in cells (Fig. 8C).

## DISCUSSION

Wnt3 is one of about 20 ligands acting in the Wnt signaling pathway and is implicated in cell proliferation, differentiation and disease. It is expressed by several signaling centers of the neural tube, including, but not limited to, the roof plate, floor plate, MHB and mid-diencephalic boundary (Clements et al., 2009). In the

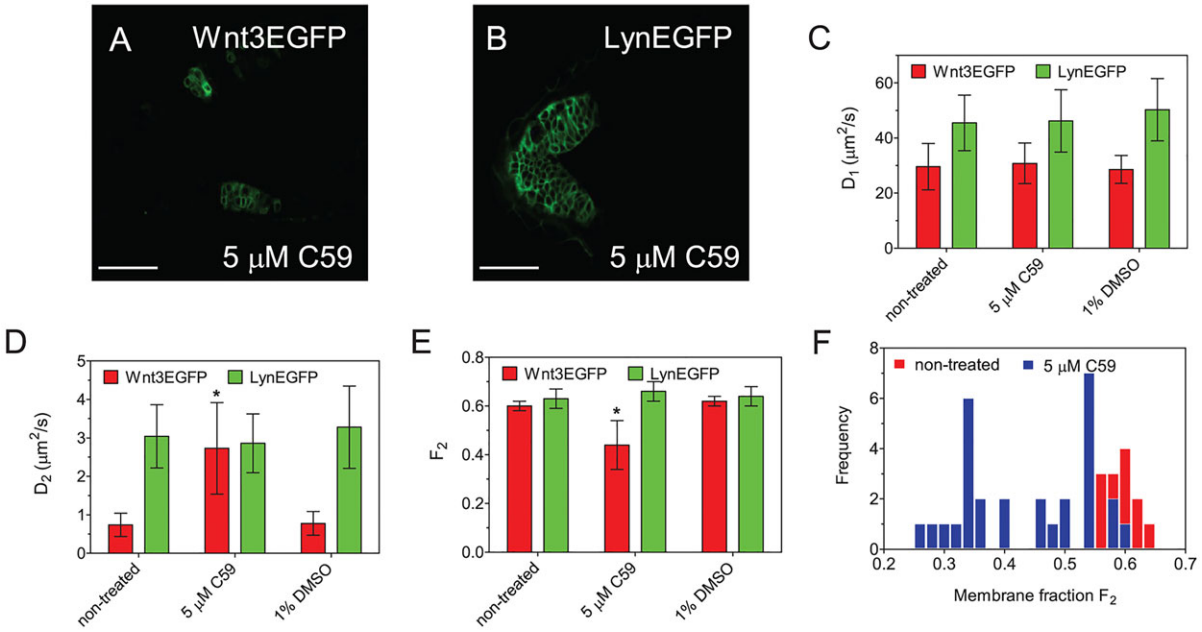


**Fig. 7. Wnt3EGFP secretion is affected by the block of Porcupine.** (A,B) Confocal images of zebrafish cerebellum expressing Wnt3EGFP and LynEGFP after C59 treatment. The embryos were treated with 5 µM C59 10-28 hpf (for details, see Materials and Methods). The samples were briefly soaked in 1× egg water before imaging in dorsal view, and FCS measurement. Scale bars: 50 µm. (C-E) Diffusion coefficients ($D_1$, $D_2$) and protein membrane distribution ($F_2$) extracted from fit at different conditions for both Wnt3EGFP and LynEGFP. (F) The results show that FCS signatures remain unchanged for LynEGFP, indicating that properties of the plasma membrane are not influenced by treatment or the drug function. Data are mean±s.d. Red bar, Wnt3EGFP; green bar, LynEGFP. Significance level, two-way *t*-test, **P*<0.001. See also Table S3.

Development (2015) 142, 3721-3733 doi:10.1242/dev.127589

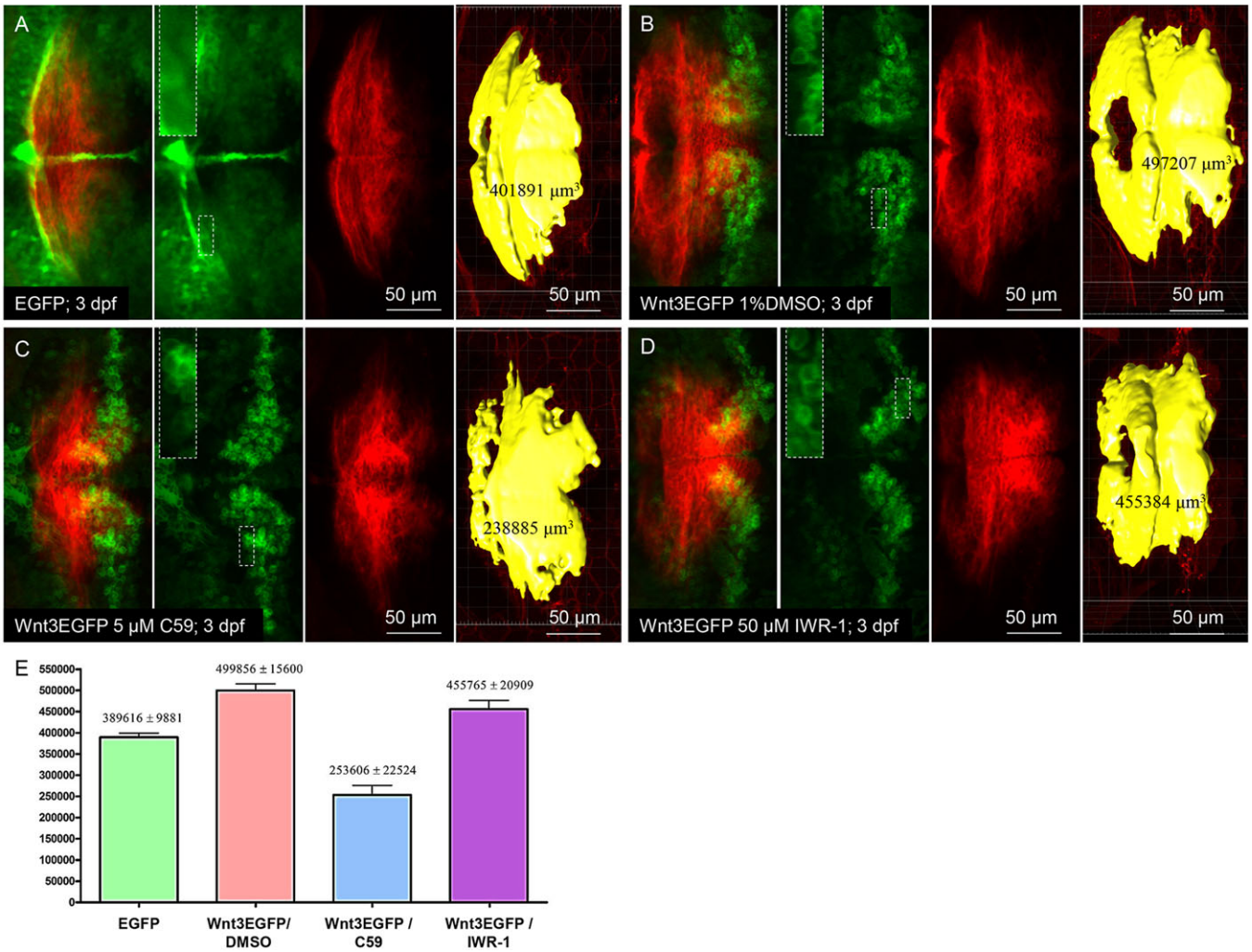


**Fig. 8. Exposure of Tg(*wnt3*:Wnt3EGFP)$^{F3}$ larvae to Wnt inhibitor C59 decreased the segmental volume of cerebellum in Tg(memKR15-16).** (A-D) *In vivo* images of 3 dpf double transgenic larvae: control Tg(*wnt3*:EGFP)$^{F1}$/Tg(memKR15-16) (A), Tg(*wnt3*:Wnt3EGFP)$^{F3}$/Tg(memKR15-16) (B-D). All Tg(*wnt3*:wnt3EGFP)$^{F3}$ double transgenic larvae were exposed to either 1% DMSO (B), 5 µM C59 (C) or 50 µM IWR-1 (D) at 36 hpf-stage for 36 h before assaying expression of fluorescent reporter at 72 hpf. High-magnification view of representative EGFP/Wnt3EGFP-expressing cells from different treatment groups (insets). KillerRed expression in the MHB and cerebellum of Tg(memKR15-16) is in red; EGFP or Wnt3EGFP expression in *wnt3* transgenics is in green; and yellow represents a 3D view of the computed volume. (E) Comparison of the resultant KillerRed-positive brain segment in Tg(memKR15-16). A significant difference was observed between segmental volumes in 1% DMSO-treated Tg(*wnt3*:Wnt3EGFP)$^{F3}$ vs C59-treated Tg(*wnt3*:Wnt3EGFP)$^{F3}$ (unpaired *t*-test, $P$=0.0001).

brain these domains encircle a large block of tissue encompassing the posterior diencephalon, midbrain and cerebellum. But could the influence of this secreted factor be experienced beyond this area? The brain ventricles adjacent to the domains of Wnt3 secretion present an opportunity for this secreted ligand to be spread in the cerebrospinal fluid (CSF) to all ventricular and central canal surfaces. Zebrafish transgenics expressing the marker EGFP in agreement with the expression pattern of *wnt3* validated the tissue-specific activity of the *wnt3* promoter (Fig. 1). The same promoter was used to generate three stable transgenic zebrafish lines expressing a functionally active fusion Wnt3EGFP protein in a tissue-specific manner (Fig. 2). Viable EGFP and Wnt3EGFP transgenic lines permitted faithful tracking of Wnt3 expression and *in vivo* characterization of its function. Conserved spatio-temporal dynamics of Wnt3EGFP fusion protein in Tg(*wnt3*:Wnt3EGFP)$^{F2}$ comparable to that of characterized EGFP reporter line Tg(*wnt3*:EGFP)$^{F1}$ allowed FCS studies of Wnt3EGFP mobility and distribution to be carried out with confidence that these reflected the mobility and distribution of endogenous Wnt3.

FCS measurements in Wnt3EGFP transgenics demonstrated the presence of several fractions of Wnt3EGFP (Fig. 9A), including two intracellular fractions – a fast-migrating intracellular fraction (Fig. 9A, i) and a slow-migrating membrane fraction (Fig. 9A, ii) – and two secreted fractions – a fast-migrating diffusing fraction (Fig. 9A, iii) and, a very slow-migrating one (Fig. 9A, iv). The bulk of Wnt3EGFP is represented by intracellular fractions, which are difficult to resolve in space because of a relatively thin layer of cytoplasm in developing cells. However, FCS provides the possibility to resolve fractions of different molecular mass by measuring mobility of proteins and their complexes. This led to the characterization of fast-migrating and slow-migrating fractions of Wnt3EGFP. The former probably represents the cytosolic fraction, and possibly some Wnt3 secreted into the extracellular space. This assumption is based on the fact that the fast-migrating fraction, which is the non-membrane-bound fraction of proteins, is larger in Wnt3 than in LynEGFP. The experiments raised the question of whether the fast-migrating fraction is a result of EGFP cleavage after Wnt3EGFP secretion. Although we cannot completely exclude

Development (2015) 142, 3721-3733 doi:10.1242/dev.127589

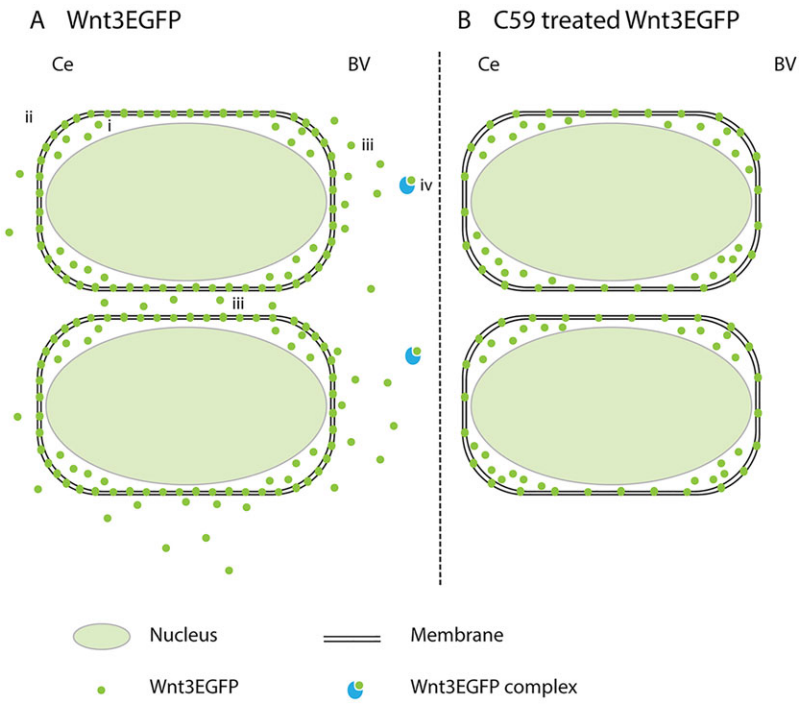


**Fig. 9. Four fractions of Wnt3EGFP in the cerebellum and brain ventricle.** (A) Schematic of the four Wnt3EGFP fractions identified: two intracellular fractions – (i) a fast-migrating intracellular fraction and (ii) a slow-migrating membrane fraction; and two secreted fractions – (iii) a fast-migrating diffusing fraction and (iv) a very slow-migrating one. (B) C59-treated Wnt3EGFP with reduced membrane-bound and secreted Wnt3EGFP. BV, brain ventricle; Ce, cerebellum.

some cleavage of EGFP from Wnt3, the fast diffusion coefficient in the brain ventricle (53.62±13.69 $\mu m^2 s^{-1}$) is still significantly slower than that of secEGFP in the same location (125.82±8.85 $\mu m^2 s^{-1}$), and thus represents at least partly intact Wnt3EGFP, possibly as small oligomers or a mixture of monomers and oligomers. These results are in line with different migration of cytosolic and membrane-bound versions of fluorescent proteins detected previously (Shi et al., 2009).

Of particular interest are the elusive secreted fractions of Wnt, including the very slow-migrating fraction of Wnt3EGFP detected in the brain ventricle. The existence of such a fraction and its high heterogeneity suggest either an aggregation of lipid-modified Wnt3EGFP (Vyas et al., 2008) or formation of complexes between Wnt3 and some extracellular matrix components, such as heparan sulphate proteoglycan (HSPG) (Kleinschmit et al., 2010), lipoprotein (Neumann et al., 2009; Mulligan et al., 2012), exosomes (Gross et al., 2012) or secreted frizzled-related proteins (Mii and Taira, 2009). A similar 'very slow' fraction of another ligand, FGF8, was previously detected by FCS (Yu et al., 2009). This is not very surprising as the activity of FGFs and Wnts both depend on evolutionarily conserved interactions with HSPG (Superina et al., 2014).

The existence of secreted fractions was supported by experiments with an inhibitor of Wnt secretion, C59, that changed Wnt3EGFP mobility at the membrane. It is known that the hydrophobicity of Wnt is reduced in the absence of Porcn owing to a block of Wnt palmitoylation (Zhai et al., 2004; Takada et al., 2006). In this situation, proteins lose membrane affinity, which could cause increased mobility of Wnt3EGFP. Post-translational palmitoylation is necessary for Wnts to be recognized and transported by Wntless (Wls) from the Golgi to the plasma membrane (Coombs et al., 2010; Herr and Basler, 2012). Therefore, Porcn inhibition causes intracellular accumulation of Wnt3EGFP and a reduction of the membrane-bound fraction. Consequently, secreted Wnt3EGFP was barely detected in the brain ventricle. The faster diffusion of Wnt3EGFP on the membrane, after partial Porcn inhibition, could be a result of a mixture of palmitoylated and non-palmitoylated Wnt3EGFP reaching the plasma membrane. In addition, previous research has shown that for some Wnt molecules, palmitoylation is necessary for raft localization (Zhai et al., 2004). The non-palmitoylated Wnt3EGFP could then reside in the more fluid-disordered liquid phase, leading to an increase in diffusion coefficient. The exact mechanism of the faster diffusion of membrane-bound non-palmitoylated Wnt3EGFP will be the topic of a future study. The reduction of the membrane-bound Wnt fraction correlated with malformed brain patterning, with a severity proportional to the temporal onset of C59-mediated inhibition of Wnt secretion. Exposure during neural plate formation led to the loss of forebrain and midbrain (Fig. S9D) in C59-treated embryos. Later drug exposure resulted in decreased cerebellum (Fig. 8C). These results support the hypothesis that Porcn is a crucial component in Wnt3 secretion. Significant variation of both mobility ($D_2$) and distribution ($F_2$) (Fig. 5F) is consistent with differential inhibitor intake by individual cells, resulting in variation of Wnt3 blocking between individual cells. However, the mobility of the fast-migrating component was not affected. This is probably because the transportation of Wnt3EGFP from ER to membrane was not blocked completely by the sub-threshold concentration of C59 used in FCS measurements.

By contrast, the inability of IWR-1 to affect Wnt3EGFP expression and secretion was expected. Unlike C59, which acts at the level of Wnt secretion, this inhibitor affects Wnt signaling in target cells at the level of downstream events of Wnt signaling mediated by β-catenin (Chen et al., 2009; Lu et al., 2009). Hence, Wnt3EGFP transgenics might not be ideal for assessing the efficacy of Wnt inhibition by IWR-1. In this respect, these transgenics complement those developed to analyze downstream effects of Wnt signaling (Moro et al., 2012). Nevertheless, the results of IWR-1 treatment emphasize the specificity of C59 action and support the existence of a secreted Wnt3 fraction.

In conclusion, several zebrafish transgenics expressing different versions of fluorescent proteins, including those of Wnt3, were developed. These tools were used for *in vivo* FCS analysis of Wnt3 migration and distribution. The measurements obtained are consistent with the existence of four fractions of Wnt3EGFP that represent the bulk of this protein in the developing brain of zebrafish: a fast-

Development (2015) 142, 3721-3733 doi:10.1242/dev.127589

migrating intracellular fraction (representing transport of expressed Wnt3 to and from the membrane), a slow-migrating membrane fraction, as well as two relatively minor secreted fractions: a fast-migrating fraction, which might represent free Wnt3, and a very slow-migrating fraction, which might represent Wnt3 in complexes with various components of the extracellular matrix. Given a significant elongation of signaling glia during late neurulation (Korzh, 2014), which probably correlates with a change in the nucleo-cytoplasm ratio, it might be of interest in future studies to compare changes in developmental dynamics and distribution of these fractions of Wnt3EGFP prior to and immediately after this dramatic morphogenetic rearrangement. The different Wnt3 transgenics will also be a useful resource for target gene profiles analysis, a topic not addressed in this publication.

## MATERIALS AND METHODS

### Molecular cloning of *wnt3* and antisense probe synthesis

A 1537 bp cDNA clone containing the full length coding region corresponding to *wnt3* (358 bp 5′UTR, 1068 ORF and 74 bp 3′UTR; NM_001114552) was amplified as a single PCR product and subcloned into pGEM-T Easy. For antisense *wnt3* probe synthesis, *wnt3*- pGEM-T Easy was first linearized with *Sal*I, followed by T7 RNA polymerase-mediated (MEGAscript, Life Technologies) transcription. Synthesized dioxygenin-labeled antisense *wnt3* probe was purified using RNA cleanup (RNeasy Mini Kit, Qiagen) before use or freezer storage.

### Generation of *wnt3* transgenic lines

BAC clone CH211-209J18 (CR749774) was purchased from BACPAC Resources Center (BACPAC Resources, USA). The following primer pair was designed to amplify DNA sequence 4000 bp upstream of ATG translational start site via PCR: *Hin*dIII_4000F, 5′-CCCAAGCTTCAAT-AAAAGAAGTGTCTGTT-3′; *Bam*HI_5′UTRW3R, 5′-CGCGGATCCG-AGGTATGTCTTGTGTGGAT-3′.

The promoter activity was first verified in promoterless vector pEGFP-1 (Clontech Laboratories, USA) and the *wnt3* promoter fragment, including the EGFP reporter, was then subcloned into miniTol2-MCS plasmid [a gift from Stephen Ekker (Balciunas et al., 2006)] at the *Hin*dIII and *Not*I sites to give the 4kbEGFP-miniTol2 recombinant plasmid.

Recombinant expression vector containing zebrafish Wnt3EGFP fusion in pEGFPN2 was generated by PCR amplification of *wnt3* open reading frame minus the stop codon with the following *Hin*dIII and *Kpn*I flanked primers: *Hin*dIII_Wnt3F, 5′-aagcttATGGATTTGTACCTGGTTGGAT-3′; *Kpn*I_Wnt3R, 5′-ggtaccaaTTTACATGTATGTACGTCGTAGA-3′. The resulting PCR amplicon was cloned into the *Hin*dIII and *Kpn*I sites of pEGFPN2.

To make the 4-kbWnt3EGFP-miniTol2 recombinant plasmid, the zebrafish *wnt3:*EGFP SV40 polyA fragment was excised from a pEGFPN2 vector backbone with *Hin*dIII and *Afe*II restriction enzymes. The fragment was blunted with Klenow and subcloned into a Klenow-blunted 4kbEGFP-miniTol2 recombinant plasmid that was previously digested with *Bam*HI and *Not*I to remove the GFP reporter.

CMV promoter-driven transient expression of Wnt3EGFP involved subcloning of the above Klenow-blunted *wnt3:*EGFP SV40 polyA fragment excised from a pEGFPN2 vector into *Eco*RV-cut pcDNA3.1(−). Recombinant CMV-Wnt3EGFP-pcDNA3.1(−) expression vector (40 pg) was injected into 1- to 4-cell stage embryos for transient expression analysis.

Stable *wnt3* promoter-driven transgenic lines were generated as stated (Balciunas et al., 2006) by co-injection of transposase mRNA and 4kbEGFP-miniTol2 or 4kbWnt3EGFP-miniTol2 to generate Tg(-4.0*wnt3*:EGFP) and Tg(-4.0*wnt3*:Wnt3EGFP) families, respectively.

### Morpholino design and injection

We obtained the same result using two different morpholino oligonucleotides directed against zebrafish *wnt3*: splice-blocking MO (MO1), 5′-CTACTCA-CCACCAGATGGGATAGCC-3′; translation blocking MO (MO2), 5′-GG-CAAAGATGGATGCTTGAGAGAAT-3′.

Morpholinos were injected into 1- to 2-cell stage embryos. The dosage used for the two different MOs were 0.2 pmol (MO1) and 0.075 pmol (MO2), respectively. Co-injection of (MO1+p53 MO) or (MO2+p53 MO) involved a 1.5-fold higher dosage of p53 MO in the MO mix.

### Zebrafish care and maintenance

Transgenic lines used in this study were: Tg(*-8.0cldnB*:lynEGFP), used for its weak membrane-tethered EGFP expression in the cerebellum (Haas and Gilmour, 2006); Tg(H2A.F/Z:EGFP), used to estimate the size of the nuclei in the cerebellum (Pauls et al., 2001); and Tg (memKR15-8) (not mapped) and Tg(memKR15-16) with membrane-tethered KillerRed expression, used as living markers of specific brain regions. Tg(memKR15-16) was mapped to the 5′UTR of *eng1b* with brain-specific expression in the midbrain–hindbrain boundary and cerebellum (Kondrychyn et al., 2011). *wnt3* promoter-driven transgenic lines generated for this study were: Tg(-4.0*wnt3*:EGFP)$^{F1}$, for spatio-temporal tracking of EGFP expression in the brain, and Tg(-4.0*wnt3*:EGFP)$^{F2}$, a weaker, but otherwise similar, EGFP reporter line used for FCS analysis. Spatio-temporally regulated Wnt3EGFP expression in the brain was studied using Tg(-4.0*wnt3*:Wnt3EGFP)$^{F1}$, Tg(-4.0*wnt3*:Wnt3EGFP)$^{F2}$ and Tg(-4.0*wnt3*:Wnt3EGFP)$^{F3}$. Transgenic adult zebrafish and embryos were obtained from the zebrafish facility in the Institute of Molecular and Cell Biology (Singapore) and staged as described (Kimmel et al., 1995; Westerfield, 2000). The Institutional Animal Care and Use Committee (IACUC) in Biological Resource Center (BRC), A*STAR, Singapore, has approved the entire study (IACUC #120787). Embryos older than 30 hpf were treated with 1-phenyl-2-thiourea at 18 hpf to prevent formation of melanin.

### Whole-mount *in situ* hybridization and immunohistochemistry

RNA *in situ* hybridization on zebrafish embryos (Oxtoby and Jowett, 1993) and two-color *in situ* hybridization (Jowett, 2001) were performed essentially as described. The NBT/BCIP-stained specimens were mounted in agar (2% Bactoagar and 5% sucrose), cryoprotected and 16 µm-thick serial cryostat sections were mounted on POLYSINE microscope slides (MICROM International) for cross-comparison the expression pattern of *wnt3* with that of EGFP in Tg(-4.0*wnt3*:EGFP)$^{F1}$. The following primary antibodies were used in immunohistochemical analyses: anti-GFAP monoclonal antibody (1:200; G3893, Sigma-Aldrich), anti-HuC/D monoclonal antibody (16A11) (1:50; A-21271, ThermoFisher Scientific), and anti-GFP antibodies mouse monoclonal antibody anti-GFP (1:200; sc-9996, Santa Cruz Biotechnology) and rabbit polyclonal anti-GFP (1:200; 632592, Clontech). Secondary antibodies used were AlexaFluor 488/594-conjugated anti-rabbit (1:500; A-11008/A-11037) or anti-mouse (1:500; A-11001/A-11005) antibodies (all from ThermoFisher Scientific). Immunodetection of GFAP was performed after fixation using HistoChoice tissue fixative (Amresco, Canada) instead of the paraformaldehyde used for all other specimens.

### Wnt inhibitors

The impact of Wnt inhibitors on brain patterning was tracked by bioimaging and FCS. Embryos at 100% epiboly or 36 hpf were exposed to 1% DMSO (control), C59 (0.1, 0.5 and 5 µM) or IWR-1 (0.5, 5 and 50 µM). Experiments were carried out in 12-well plates (Falcon BD Biosciences) with 20 embryos and 1.5 ml of the respective solutions per well. All solutions of Wnt inhibitors contain 1% DMSO. Embryos treated at 100 % epiboly were incubated in these solutions until FCS imaging at 28 hpf or confocal imaging at 48 hpf. Embryos treated at 36 hpf were incubated in these solutions until confocal imaging at 72 hpf.

### Microscopy

*In vivo* fluorescent images were acquired with an upright laser scanning microscope (LSM) Meta 510 (Carl Zeiss) equipped with an Achroplan long working distance dipping objective (40×, NA 0.75W; Carl Zeiss) using two laser lines (488/543 nm). All imaging was performed at room temperature (24°C). The photomicrographs were taken with an AxioCam HRC digital camera (Carl Zeiss Vision).

Development (2015) 142, 3721-3733 doi:10.1242/dev.127589

### Intensity line profiles

Fluorescent images were acquired with an Olympus FV 300 confocal microscope (Olympus) equipped with a water-immersion objective (60×, NA 1.2; Olympus). Excitation was provided by the 488-nm laser line of an Argon ion laser. All imaging was performed at room temperature (24°C). ImageJ was used to generate intensity profiles of cerebellar cells at a boundary of the brain ventricle. Data was normalized and aligned to the highest intensity point. The following transgenic larvae were used for the image acquisition and data analysis pertaining to the intensity profiles: Tg(-*8.0cldnB*:lynEGFP); Tg(-4.0*wnt3*:Wnt3EGFP)$^{F2}$ transgenic embryos. Microinjection of secEGFP mRNA (a gift from Prof. Karuna Sampath, Temasek Life Science Laboratory, Singapore) into 1- to 2-cell blastula staged embryos was followed by selecting secGFP-positive embryos at 30 hpf for intensity profile scans at 34 hpf. Plots are the average value from three embryos.

## Fluorescence correlation spectroscopy (FCS)

The FCS setup was described previously in detail (Pan et al., 2007a). Briefly, FCS was performed using a customized Olympus FV 300 confocal microscope. Excitation was provided by the 488 nm laser line of an Argon ion laser focused into samples by a water-immersion objective (60×, NA 1.2; Olympus). The laser power, measured before the objective, was 15 µW. The emitted light, which passed an internal 3× magnification stage in the confocal microscope, passed through a 150 µm pinhole, then was focused through band-pass filters 513/17-25 (Semrock, Rochester, NY, USA), onto avalanche-photodiode detector (SPCM-AQR-14; Pacer, Berkshire, UK). Autocorrelation curves were computed online using a hardware correlator (Flex02-01D; Correlator.com, Bridgewater, NJ, USA). Curve fitting was performed by a self-written program in Igor Pro 6.0 (WaveMetrics, Lake Oswego, OR, USA). For further details on FCS, including theory and fitting models, please see the supplementary materials and methods.

### Acknowledgements

C59 was kindly provided by Drs May Ann Lee, Zhiyuan Ke (Experimental Therapeutics Centre, A*STAR, Singapore) and David Virshup (Program in Cancer and Stem Cell Biology, Duke-NUS Graduate Medical School, Singapore).

### Competing interests

The authors declare no competing or financial interests.

### Author contributions

C.T. designed and generated the *wnt3* promoter-driven transgenic lines, conducted *in vivo* analysis of *wnt3* transgenics and wrote the paper; G.S. designed and performed the FCS experiments, analyzed the data and wrote the paper; H.S. made the recombinant CMV-Wnt3EGFP construct and validated its activity in zebrafish; V.K. and T.W. designed the experiments, supervised the work, wrote and approved the paper.

### Funding

G.S. was supported by a National University of Singapore scholarship. T.W. gratefully acknowledges funding by a grant from the Singapore Ministry of Education [MOE2012-T2-1-101, R-154-000-543-112]. V.K., H.S. and C.T. are supported by an Institute of Molecular and Cell Biology institutional grant from the Agency for Science, Technology, and Research (A*STAR) of Singapore. V.K. and C.T. are also supported by an A*STAR Nutrition and Food Science grant [1121770041].

### Supplementary information

Supplementary information available online at
http://dev.biologists.org/lookup/suppl/doi:10.1242/dev.127589/-/DC1

### References

**Anastas, J. N. and Moon, R. T.** (2013). WNT signalling pathways as therapeutic targets in cancer. *Nat. Rev. Cancer* **13**, 11-26.

**Anne, S. L., Govek, E.-E., Ayrault, O., Kim, J. H., Zhu, X., Murphy, D. A., Van Aelst, L., Roussel, M. F. and Hatten, M. E.** (2013). WNT3 inhibits cerebellar granule neuron progenitor proliferation and medulloblastoma formation via MAPK activation. *PLoS ONE* **8**, e81769.

**Balciunas, D., Wangensteen, K. J., Wilber, A., Bell, J., Geurts, A., Sivasubbu, S., Wang, X., Hackett, P. B., Largaespada, D. A., McIvor, R. S. et al.** (2006). Harnessing a high cargo-capacity transposon for genetic applications in vertebrates. *PLoS Genet.* **2**, 1715-1724.

**Blader, P., Strähle, U. and Ingham, P. W.** (1996). Three Wnt genes expressed in a wide variety of tissues during development of the zebrafish, Danio rerio: developmental and evolutionary perspectives. *Dev. Genes Evol.* **206**, 3-13.

**Bonner, J., Gribble, S. L., Veien, E. S., Nikolaus, O. B., Weidinger, G. and Dorsky, R. I.** (2008). Proliferation and patterning are mediated independently in the dorsal spinal cord downstream of canonical Wnt signaling. *Dev. Biol.* **313**, 398-407.

**Bulfone, A., Puelles, L., Porteus, M. H., Frohman, M. A., Martin, G. R. and Rubenstein, J. L.** (1993). Spatially restricted expression of Dlx-1, Dlx-2 (Tes-1), Gbx-2, and Wnt-3 in the embryonic day 12.5 mouse forebrain defines potential transverse and longitudinal segmental boundaries. *J. Neurosci.* **13**, 3155-3172.

**Chen, B., Dodge, M. E., Tang, W., Lu, J., Ma, Z., Fan, C.-W., Wei, S. G., Hao, W., Kilgore, J., Williams, N. S. et al.** (2009). Small molecule–mediated disruption of Wnt-dependent signaling in tissue regeneration and cancer. *Nat. Chem. Biol.* **5**, 100-107.

**Clements, W. K., Ong, K. G. and Traver, D.** (2009). Zebrafish wnt3 is expressed in developing neural tissue. *Dev. Dyn.* **238**, 1788-1795.

**Clevers, H. and Nusse, R.** (2012). Wnt/beta-catenin signaling and disease. *Cell* **149**, 1192-1205.

**Coombs, G. S., Yu, J., Canning, C. A., Veltri, C. A., Covey, T. M., Cheong, J. K., Utomo, V., Banerjee, N., Zhang, Z. H., Jadulco, R. C. et al.** (2010). WLS-dependent secretion of WNT3A requires Ser209 acylation and vacuolar acidification. *J. Cell Sci.* **123**, 3357-3367.

**Dorsky, R. I., Sheldahl, L. C. and Moon, R. T.** (2002). A transgenic Lef1/beta-catenin-dependent reporter is expressed in spatially restricted domains throughout zebrafish development. *Dev. Biol.* **241**, 229-237.

**Foo, Y. H., Korzh, V. and Wohland, T.** (2012). Fluorescence correlation and cross-correlation spectroscopy using fluorescent proteins for measurements of biomolecular processes in living organisms. *Fluoresc. Protein. II* **12**, 213-248.

**Garriock, R. J., Warkman, A. S., Meadows, S. M., D'Agostino, S. and Krieg, P. A.** (2007). Census of vertebrate Wnt genes: isolation and developmental expression of Xenopus Wnt2, Wnt3, Wnt9a, Wnt9b, Wnt10a, and Wnt16. *Dev. Dyn.* **236**, 1249-1258.

**Gross, J. C., Chaudhary, V., Bartscherer, K. and Boutros, M.** (2012). Active Wnt proteins are secreted on exosomes. *Nat. Cell Biol.* **14**, 1036-1045.

**Guo, S.-M., He, J., Monnier, N., Sun, G., Wohland, T. and Bathe, M.** (2012). Bayesian approach to the analysis of fluorescence correlation spectroscopy data II: application to simulated and in vitro data. *Anal. Chem.* **84**, 3880-3888.

**Hashimoto, M. and Hibi, M.** (2012). Development and evolution of cerebellar neural circuits. *Dev. Growth Differ.* **54**, 373-389.

**Herr, P. and Basler, K.** (2012). Porcupine-mediated lipidation is required for Wnt recognition by Wls. *Dev. Biol.* **361**, 392-402.

**Jessell, T. M.** (2000). Neuronal specification in the spinal cord: Inductive signals and transcriptional codes. *Nat. Rev. Genet.* **1**, 20-29.

**Jowett, T.** (2001). Double in situ hybridization techniques in zebrafish. *Methods* **23**, 345-358.

**Kaslin, J., Kroehne, V., Benato, F., Argenton, F. and Brand, M.** (2013). Development and specification of cerebellar stem and progenitor cells in zebrafish: from embryo to adult. *Neural Dev.* **8**, 9.

**Kim, M., Lee, H. C., Tsedensodnom, O., Hartley, R., Lim, Y.-S., Yu, E., Merle, P. and Wands, J. R.** (2008). Functional interaction between Wnt3 and Frizzled-7 leads to activation of the Wnt/beta-catenin signaling pathway in hepatocellular carcinoma cells. *J. Hepatol.* **48**, 780-791.

**Kimmel, C. B., Ballard, W. W., Kimmel, S. R., Ullmann, B. and Schilling, T. F.** (1995). Stages of embryonic development of the zebrafish. *Dev. Dyn.* **203**, 253-310.

**Kleinschmit, A., Koyama, T., Dejima, K., Hayashi, Y., Kamimura, K. and Nakato, H.** (2010). Drosophila heparan sulfate 6-O endosulfatase regulates Wingless morphogen gradient formation. *Dev. Biol.* **345**, 204-214.

**Kobune, M., Chiba, H., Kato, J., Kato, K., Nakamura, K., Kawano, Y., Takada, K., Takimoto, R., Takayama, T., Hamada, H. et al.** (2007). Wnt3/RhoA/ROCK signaling pathway is involved in adhesion-mediated drug resistance of multiple myeloma in an autocrine mechanism. *Mol. Cancer Ther.* **6**, 1774-1784.

**Kondrychyn, I., Teh, C., Garcia-Lecea, M., Guan, Y., Kang, A. and Korzh, V.** (2011). Zebrafish enhancer TRAP transgenic line database ZETRAP 2.0. *Zebrafish* **8**, 181-182.

**Kondrychyn, I., Teh, C., Sin, M. and Korzh, V.** (2013). Stretching morphogenesis of the roof plate and formation of the central canal. *PLoS ONE* **8**, e56219.

**Korzh, V.** (2014). Stretching cell morphogenesis during late neurulation and mild neural tube defects. *Dev. Growth Differ.* **56**, 425-433.

**Korzh, V., Kondrichin, I. and García-Lecea, M.** (2007). Gliogenesis in zebrafish. In *Trends in Glial Research-Basic and Applied* (ed. S.T. Dheen and E.A. Ling), pp. 81-98. Trivandrum-695 023, Kerala, India: Research Signpost.

**Krauss, S., Korzh, V., Fjose, A. and Johansen, T.** (1992). Expression of four zebrafish wnt-related genes during embryogenesis. *Development* **116**, 249-259.

**Lancaster, M. A., Gopal, D. J., Kim, J., Saleem, S. N., Silhavy, J. L., Louie, C. M., Thacker, B. E., Williams, Y., Zaki, M. S. and Gleeson, J. G.** (2011). Defective Wnt-dependent cerebellar midline fusion in a mouse model of Joubert syndrome. *Nat. Med.* **17**, 726-731.

**Liu, P. T., Wakamiya, M., Shea, M. J., Albrecht, U., Behringer, R. R. and Bradley, A.** (1999). Requirement for Wnt3 in vertebrate axis formation. *Nat. Genet.* **22**, 361-365.
**Lu, J., Ma, Z., Hsieh, J.-C., Fan, C.-W., Chen, B. Z., Longgood, J. C., Williams, N. S., Amatruda, J. F., Lum, L. and Chen, C.** (2009). Structure–activity relationship studies of small-molecule inhibitors of Wnt response. *Bioorg. Med. Chem. Lett.* **19**, 3825-3827.
**Macháň, R. and Wohland, T.** (2014). Recent applications of fluorescence correlation spectroscopy in live systems. *FEBS Lett.* **588**, 3571-3584.
**Mii, Y. and Taira, M.** (2009). Secreted Frizzled-related proteins enhance the diffusion of Wnt ligands and expand their signalling range. *Development* **136**, 4083-4088.
**Millen, K. J., Hui, C. C. and Joyner, A. L.** (1995). A role for En-2 and other murine homologues of Drosophila segment polarity genes in regulating positional information in the developing cerebellum. *Development* **121**, 3935-3945.
**Molven, A., Njolstad, P. R. and Fjose, A.** (1991). Genomic structure and restricted neural expression of the zebrafish wnt-1 (int-1) gene. *EMBO J.* **10**, 799-807.
**Moro, E., Ozhan-Kizil, G., Mongera, A., Beis, D., Wierzbicki, C., Young, R. M., Bournele, D., Domenichini, A., Valdivia, L. E., Lum, L. et al.** (2012). In vivo Wnt signaling tracing through a transgenic biosensor fish reveals novel activity domains. *Dev. Biol.* **366**, 327-340.
**Muller, P., Rogers, K. W., Yu, S. R., Brand, M. and Schier, A. F.** (2013). Morphogen transport. *Development* **140**, 1621-1638.
**Mulligan, K. A., Fuerer, C., Ching, W., Fish, M., Willert, K. and Nusse, R.** (2012). Secreted Wingless-interacting molecule (Swim) promotes long-range signaling by maintaining Wingless solubility. *Proc. Natl. Acad. Sci. USA* **109**, 370-377.
**Mütze, J., Ohrt, T. and Schwille, P.** (2011). Fluorescence correlation spectroscopy in vivo. *Laser Photonics Rev.* **5**, 52-67.
**Neumann, S., Coudreuse, D. Y. M., van der Westhuyzen, D. R., Eckhardt, E. R. M., Korswagen, H. C., Schmitz, G. and Sprong, H.** (2009). Mammalian Wnt3a is released on lipoprotein particles. *Traffic* **10**, 334-343.
**Niemann, S., Zhao, C., Pascu, F., Stahl, U., Aulepp, U., Niswander, L., Weber, J. L. and Müller, U.** (2004). Homozygous WNT3 mutation causes tetra-amelia in a large consanguineous family. *Am. J. Hum. Genet.* **74**, 558-563.
**Nusse, R. and Varmus, H. E.** (1982). Many tumors induced by the mouse mammary tumor virus contain a provirus integrated in the same region of the host genome. *Cell* **31**, 99-109.
**Nusse, R. and Varmus, H.** (2012). Three decades of Wnts: a personal perspective on how a scientific field developed. *EMBO J.* **31**, 2670-2684.
**Pan, X., Foo, W., Lim, W., Fok, M. H. Y., Liu, P., Yu, H., Maruyama, I. and Wohland, T.** (2007a). Multifunctional fluorescence correlation microscope for intracellular and microfluidic measurements. *Rev. Sci. Instrum.* **78**, 053711.
**Pan, X., Yu, H., Shi, X., Korzh, V. and Wohland, T.** (2007b). Characterization of flow direction in microchannels and zebrafish blood vessels by scanning fluorescence correlation spectroscopy. *J. Biomed. Opt.* **12**, 014034.
**Park, H.-C., Kim, C.-H., Bae, Y.-K., Yeo, S.-Y., Kim, S.-H., Hong, S.-K., Shin, J., Yoo, K.-W., Hibi, M., Hirano, T. et al.** (2000). Analysis of upstream elements in the HuC promoter leads to the establishment of transgenic zebrafish with fluorescent neurons. *Dev. Biol.* **227**, 279-293.
**Pauls, S., Geldmacher-Voss, B. and Campos-Ortega, J. A.** (2001). A zebrafish histone variant H2A.F/Z and a transgenic H2A.F/Z:GFP fusion protein for in vivo studies of embryonic development. *Dev. Genes Evol.* **211**, 603-610.
**Proffitt, K. D., Madan, B., Ke, Z., Pendharkar, V., Ding, L., Lee, M. A., Hannoush, R. N. and Virshup, D. M.** (2013). Pharmacological inhibition of the Wnt acyltransferase PORCN prevents growth of WNT-driven mammary cancer. *Cancer Res.* **73**, 502-507.
**Ries, J., Yu, S. R., Burkhardt, M., Brand, M. and Schwille, P.** (2009). Modular scanning FCS quantifies receptor-ligand interactions in living multicellular organisms. *Nat. Methods* **6**, 643-645.
**Robu, M. E., Larson, J. D., Nasevicius, A., Beiraghi, S., Brenner, C., Farber, S. A. and Ekker, S. C.** (2007). p53 activation by knockdown technologies. *PLoS Genet.* **3**, e78.
**Roelink, H. and Nusse, R.** (1991). Expression of two members of the Wnt family during mouse development-restricted temporal and spatial patterns in the developing neural tube. *Genes Dev.* **5**, 381-388.
**Selvadurai, H. J. and Mason, J. O.** (2011). Wnt/beta-catenin signalling is active in a highly dynamic pattern during development of the mouse cerebellum. *PLoS ONE* **6**, e23012.
**Shi, X., Shin Teo, L., Pan, X., Chong, S.-W., Kraut, R., Korzh, V. and Wohland, T.** (2009). Probing events with single molecule sensitivity in zebrafish and Drosophila embryos by fluorescence correlation spectroscopy. *Dev. Dyn.* **238**, 3156-3167.
**Stanganello, E., Hagemann, A. I. h., Mattes, B., Sinner, C., Meyen, D., Weber, S., Schug, A., Raz, E. and Scholpp, S.** (2015). Filopodia-based Wnt transport during vertebrate tissue patterning. *Nat. Commun.* **6**, 5846.
**Stewart, S., Gomez, A. W., Armstrong, B. E., Henner, A. and Stankunas, K.** (2014). Sequential and opposing activities of Wnt and BMP coordinate zebrafish bone regeneration. *Cell Rep.* **6**, 482-498.
**Sun, G., Guo, S.-M., Teh, C., Korzh, V., Bathe, M. and Wohland, T.** (2015). Bayesian model selection applied to the analysis of fluorescence correlation spectroscopy data of fluorescent proteins in vitro and in vivo. *Anal. Chem.* **87**, 4326-4333.
**Superina, S., Borovina, A. and Ciruna, B.** (2014). Analysis of maternal-zygotic ugdh mutants reveals divergent roles for HSPGs in vertebrate embryogenesis and provides new insight into the initiation of left–right asymmetry. *Dev. Biol.* **387**, 154-166.
**Takada, R., Satomi, Y., Kurata, T., Ueno, N., Norioka, S., Kondoh, H., Takao, T. and Takada, S.** (2006). Monounsaturated fatty acid modification of Wnt protein: Its role in Wnt secretion. *Dev. Cell* **11**, 791-801.
**Tanaka, K., Okabayashi, K., Asashima, M., Perrimon, N. and Kadowaki, T.** (2000). The evolutionarily conserved porcupine gene family is involved in the processing of the Wnt family. *Euro. J. Biochem.* **267**, 4300-4311.
**van de Water, S., van de Wetering, M., Joore, J., Esseling, J., Bink, R., Clevers, H. and Zivkovic, D.** (2001). Ectopic Wnt signal determines the eyeless phenotype of zebrafish masterblind mutant. *Development* **128**, 3877-3888.
**Vyas, N., Goswami, D., Manonmani, A., Sharma, P., Ranganath, H. A., VijayRaghavan, K., Shashidhara, L. S., Sowdhamini, R. and Mayor, S.** (2008). Nanoscale organization of Hedgehog is essential for long-range signaling. *Cell* **133**, 1214-1227.
**Westerfield, M.** (2000). The Zebrafish Book. Eugene: University of Oregon Press.
**Willert, K., Brown, J. D., Danenberg, E., Duncan, A. W., Weissman, I. L., Reya, T., Yates, J. R. and Nusse, R.** (2003). Wnt proteins are lipid-modified and can act as stem cell growth factors. *Nature* **423**, 448-452.
**Ye, W., Shimamura, K., Rubenstein, J. L. R., Hynes, M. A. and Rosenthal, A.** (1998). FGF and Shh signals control dopaminergic and serotonergic cell fate in the anterior neural plate. *Cell* **93**, 755-766.
**Ye, W., Bouchard, M., Stone, D., Liu, X. D., Vella, F., Lee, J., Nakamura, H., Ang, S.-L., Busslinger, M. and Rosenthal, A.** (2001). Distinct regulators control the expression of the mid-hindbrain organizer signal FGF8. *Nat. Neurosci.* **4**, 1175-1181.
**Yin, A., Korzh, V. and Gong, Z.** (2012). Perturbation of zebrafish swimbladder development by enhancing Wnt signaling in Wif1 morphants. *Biochim. Biophys. Acta* **1823**, 236-244.
**Yu, S. R., Burkhardt, M., Nowak, M., Ries, J., Petrášek, Z., Scholpp, S., Schwille, P. and Brand, M.** (2009). Fgf8 morphogen gradient forms by a source-sink mechanism with freely diffusing molecules. *Nature* **461**, 533-536.
**Zhai, L., Chaturvedi, D. and Cumberledge, S.** (2004). Drosophila Wnt-1 undergoes a hydrophobic modification and is targeted to lipid rafts, a process that requires porcupine. *J. Biol. Chem.* **279**, 33220-33227.
**Zhou, S., Lo, W.-C., Suhalim, J. L., Digman, M. A., Gratton, E., Nie, Q. and Lander, A. D.** (2012). Free extracellular diffusion creates the Dpp morphogen gradient of the drosophila wing disc. *Curr. Biol.* **22**, 668-675.